p-Type Electrical Transport of Chemically Doped Epitaxial Graphene Nanoribbons

Sarah E. Bryan, Kevin Brenner, Yinxiao Yang, Raghun Murali, *Member, IEEE*, and James D. Meindl, *Life Fellow, IEEE*

***Abstract*—We present the first demonstration of p-type electrical transport in chemically doped epitaxial graphene (EG) nanoribbons produced on silicon carbide (SiC). The thermal annealing of cross-linked thin films of hydrogen silsesquioxane (HSQ) is found to be capable of overcoming intrinsic n-type doping from the SiC substrate, resulting in p-type functionality. A smooth transition from n- to p-type carriers, spanning a Fermi shift of ∼0.45 eV, is observed by controlling the density and chemical composition of HSQ. This technique provides a route for complementary transistor and interconnect fabrication, as well as facilitating chemically doped p-n junctions in EG.**

***Index Terms*—Chemical doping, epitaxial graphene (EG), graphene nanoribbons, p-type transport.**

I. Introduction

THE superior electrical and thermal properties of graphene make it a viable candidate for future nanoelectronic devices, with growth on silicon carbide (SiC) providing one of the most promising routes to large-scale production. For epitaxial graphene (EG) to function in a complementary manner, parallel to metal–oxide–semiconductor (CMOS) devices, the ability to fabricate n- and p-type regions is necessary. The realization of a number of promising device architectures in graphene relies on p-n junction formation [1], furthering the need for a reliable complementary doping technique. In addition, the possibility of a monolithic system based on EG [2], where the transistor and the interconnect material are seamlessly integrated, would require complementary doping to avoid unintentional p-n junction formation at the transistor–interconnect interface. The major barrier to creating p-n junctions with EG is the intrinsic n-type doping of the material due to the SiC substrate [3], which pins the Fermi level ∼0.4 eV above the Dirac point.

EG grown on the Si-terminated face (0001) of SiC consists of an interface layer that is structurally similar to monolayer graphene but contains a large percentage of carbon atoms bound to the Si atoms below [4]; the result is a buffer layer that does not possess the electronic properties of graphene. Subsequent graphene monolayers that exhibit the unique linear E-k spectrum characteristic of graphene grow on top of the buffer layer and are intrinsically heavily n-doped. A variety of methods have been employed to counteract the n-doping of EG, with most experimental evidence being obtained on large-area graphene via spectroscopic studies that provide limited insight into electrical transport properties. Intercalation of H atoms has been shown to saturate dangling bonds from Si atoms in the SiC substrate, effectively creating a freestanding graphene monolayer [5] that exhibits charge neutrality after annealing. Similarly, Au atoms have been used in an intercalation process [6] to shift the Fermi level closer to the Dirac point in EG. Weak hole injection into EG has been also accomplished through surface adsorption of gas molecules [7] such as NO_2. In addition, noncovalent functionalization using aromatic molecules has succeeded in shifting the Fermi level to the Dirac point [8]. Controlled and tunable p-type doping of EG nanoribbons (GNRs) resulting in a shift of the Fermi level below the Dirac point has not yet been achieved in these studies [5]–[8]. In this letter, we use a thin-film dielectric coating to demonstrate the first electrical transport measurements of p-type epitaxial GNRs, enabling CMOS functionality in EG. Developing a methodology to selectively dope epitaxial GNRs, as opposed to large-area graphene, is extremely important for digital logic applications because it can be used to build complementary devices, induce a bandgap in graphene [9], and explore many novel device concepts based on graphene p-n junctions.

II. Experiment

EG was grown on semi-insulating 4H–SiC (Cree, Inc.) substrates in a radio-frequency induction furnace at a temperature range from 1600 °C to 1800 °C and a pressure of $\sim 10^{-5}$ torr for 10 min. Prior to growth, SiC substrates were hydrogen etched for 30 min at 1400 °C to remove chemical-mechanical polishing damage. Atomic force microscopy (AFM) performed immediately after growth revealed the characteristic morphology of EG on SiC (0001) [see Fig. 1(a)]. Raman spectroscopy was used to verify the presence of monolayer graphene.[1] Hall measurements of as-grown EG $(3.5 \times 3.5\ \text{mm}^2)$ revealed an average sheet carrier density of $\sim 10^{13}\ \text{cm}^{-2}$ and average mobility of $2500\ \text{cm}^2/\text{V} \cdot \text{s}$.

Electron-beam (e-beam) lithography was used to pattern the contact electrodes, followed by e-beam evaporation of a 20/80-nm Ti/Au stack. Resist residue removal after liftoff

Manuscript received February 6, 2012; revised February 23, 2012; accepted February 25, 2012. Date of publication April 4, 2012; date of current version May 18, 2012. This work was supported in part by the National Science Foundation under Grant ECCS 1001986. The review of this letter was arranged by Editor A. Ortiz-Conde.

The authors are with the Nanotechnology Research Center, Georgia Institute of Technology, Atlanta, GA 30332 USA (e-mail: sebryan@gatech.edu).

Color versions of one or more of the figures in this letter are available online at http://ieeexplore.ieee.org.

Digital Object Identifier 10.1109/LED.2012.2189432

[1]SEM imaging was performed after GNR fabrication to determine which GNR devices were confined on a single SiC terrace. This way, regions of thicker graphene close to the terrace step edge were avoided. GNR devices found to cross terrace step edges (i.e., regions of thicker graphene) were not included in this study.

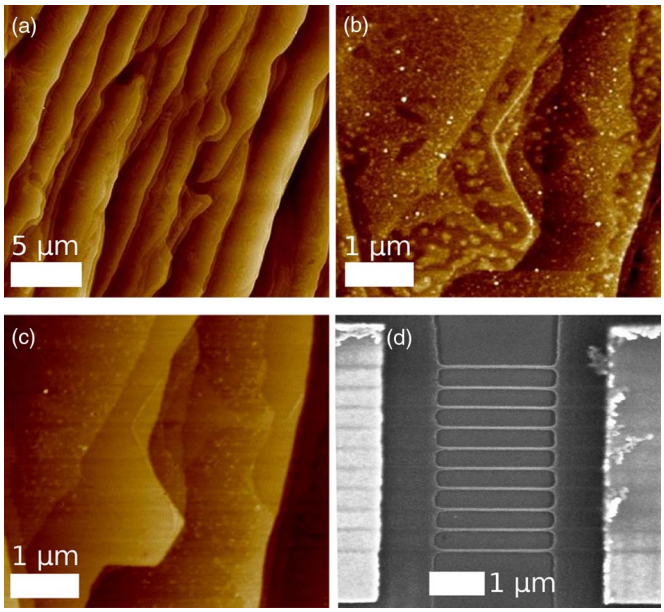

Fig. 1. (a) AFM scan of EG on SiC (0001). (b) AFM scan of resist residues on graphene after electrode fabrication. (c) Identical region in (b) after Ar/H_2 anneal showing significant improvement in surface roughness. (d) SEM image of 20-nm GNRs coated with HSQ.

was necessary to obtain a clean pristine basal plane; this was accomplished by a thermal anneal at 330 °C (P $\sim$ 4 torr) for 3 h in an environment of Ar/H_2 (3800/200 sccm). A significant improvement in surface roughness was achieved after the anneal [see Fig. 1(b) and (c)]. GNRs were patterned in a 30-nm-thick film of hydrogen silsesquioxane (HSQ) and transferred into the graphene using an Ar plasma [see Fig. 1(d)]. The top-gate structure was composed of 100 nm of e-beam evaporated SiO_2 on top of the HSQ-coated GNRs, plus a 20/80-nm Ti/Au gate stack. The gate width of 2.1 μm completely covered the GNRs ($L = 2$ μm, $W = 20$ nm), and the leakage current monitored during testing did not exceed 10 nA. Immediately after fabrication, samples were loaded into a cryogenic probe station and pumped down to P $= 1.5 \times 10^{-6}$ torr. Four-point electrical measurements ($V_{DS} = 2$ V, $T = 77$ K) were performed to eliminate contact resistance. A pulsed gate bias technique was used to minimize hysteresis and allow for precise extraction of the doping level [10].

III. Results and Discussion

As-fabricated devices, before the HSQ etch mask is annealed, show a negative minimum conductivity point ($V_{G\min}$) of -54 V, corresponding to an n-type carrier density of $\sim 1.1 \times 10^{13}$ cm^{-2} [see Fig. 2(a)]. After the initial electrical testing, samples were annealed on a hotplate in the ambient environment at 250 °C for 24, 48, and 72 h; samples were then loaded into the cryogenic probe station and allowed to pump down overnight before electrical testing. After 72 h of annealing, $V_{G\min}$ for the three devices has shifted by more than $+50$ V to positive gate voltages ($V_{G\min} = +3$ V), indicating a p-type carrier density of $\sim 6.5 \times 10^{11}$ cm^{-2} in the GNRs [see Fig. 2(a)]. Extended annealing beyond 72 h did not result in any further shifts of $V_{G\min}$ or changes to the I–V curves,

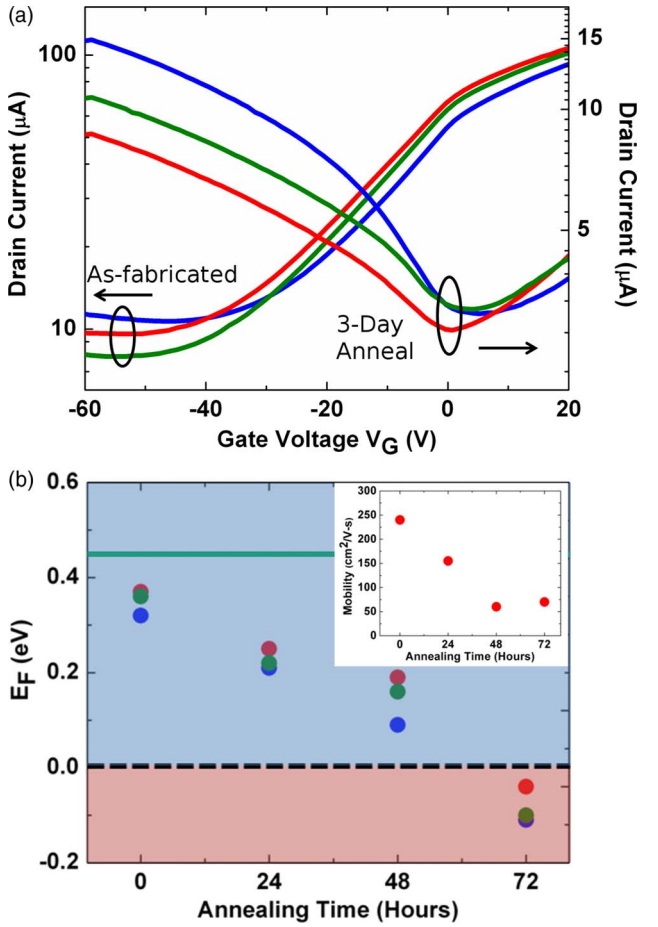

Fig. 2. (a) I–V data for three identical devices. The minimum conductivity point ($V_{G\min}$) is negative directly after fabrication; annealing for 72 h leads to a strong positive shift of $V_{G\min}$. (b) The Fermi level is plotted as a function of annealing time. A 72-h anneal results in a shift of $V_{G\min}$ beyond the Dirac point ($E_D = E_F$). The (solid) green band represents the Fermi level for intrinsically n-doped EG on SiC (0001). The (dashed) black band represents the Dirac point. The inset shows a plot of the average mobility for the three devices as a function of annealing time.

suggesting that all available dangling O bonds in the HSQ thin film have been allowed to contact the graphene surface. In addition, repeated electrical testing after samples were removed from vacuum and left in the ambient for two weeks showed no significant changes to the I–V curves, suggesting that the HSQ doping method presented herein is stable.

When energy is delivered to the HSQ thin film, the material undergoes a transition from a cagelike to a networklike structure via the scission of Si–H bonds [11]. For the e-beam doses used to pattern the GNRs, the number of Si–H bonds in the HSQ film is expected [12] to be reduced by $\sim$75%, resulting in the formation of volatile molecular H_2, which is removed from the film via out gassing; the result is an O-rich film. HSQ has been shown to dope exfoliated graphene flakes [13] either n- or p-type with strong dependence on e-beam irradiation and plasma exposure time; however, the intrinsic n-type doping of EG makes p-type doping more challenging. In this letter, we use thermal annealing to modify the density of cross-linked HSQ thin films atop EG, resulting in a further enhancement of the basal plane p-type doping. The annealing temperature is kept in a range where only a structural change in the film is expected [14], resulting in increased film

density and reduced porosity [15]. The increased density of the O-rich film allows more O atoms to contact the surface, allowing for charge transfer to occur between graphene and oxygen. The result is p-type doping of EG, accompanied by charged-impurity scattering. The modification of the density of the HSQ film is the key to producing sufficient basal plane doping to overcome the n-type doping from the SiC substrate. Other basal plane techniques that rely on adsorption of molecules or less dense film coatings fail to provide enough basal plane dopants and are thus incapable of producing p-type EG.

The mobility of the GNR is extracted using the Drude conductivity relation, i.e., $\sigma = q\mu n_{\rm elec}$, where σ is evaluated at a set reference carrier density of 9.94×10^{12} cm^{-2}. For the GNRs in this work, testing of as-fabricated devices yielded $\mu = 240$ cm^2/V $\cdot$ s. The mobility reduction from the as-grown value of 2500 cm^2/V $\cdot$ s is mostly attributed to the size effect [16] for the devices presented in this work, although changes in carrier concentration also strongly affect graphene mobility [17]. Work based on nongated HSQ-coated GNRs predicts a mobility range of 100–500 cm^2/V $\cdot$ s for a 20-nm GNR.

After annealing of HSQ for 72 h, the mobility is seen to further reduce to $\mu = 70$ cm^2/V $\cdot$ s. For charged-impurity scattering in graphene, the mobility, value of minimum conductivity ($\sigma_{\rm min}$), and $I_{\rm on}/I_{\rm off}$ ratio are all expected to reduce as a function of doping [18]. The samples tested in this work show a reduction in mobility by 70%, a decrease in minimum conductivity by 60%–80%, and a change in the $I_{\rm on}/I_{\rm off}$ ratio from 8 to 3.5 after 72 h of HSQ annealing. We suggest that the charged-impurity scattering in our samples is directly attributed to the increased number of dopants in contact with the basal plane as the density of the HSQ film increases. Since the basal plane of the GNRs is passivated by the HSQ film and the top-gate dielectric, negligible p-type doping or changes in mobility due to atmospheric adsorbates is expected.

To determine the Fermi energy corresponding to the location of $V_{G\rm min}$, the relation [19] $E_F(n) = {\rm sgn}(n)\hbar v_F\sqrt{\pi|n|}$ ($v_F =$ Fermi velocity $= 1 \times 10^8$ cm/s, $n =$ carrier density evaluated at the Dirac point) was used. According to [20], the 2-D density of states is accurate for this calculation at an operating voltage of ± 2 V. Fringe field effects for a 20-nm GNR were accounted for in the determination of the carrier density via COMSOL simulations. Fig. 2(b) displays the negative Fermi level shift, indicating p-type doping of EG.

IV. Conclusion

In conclusion, the first electrical transport measurements of chemically doped p-type EG on SiC have been presented. It is shown that the minimum conductivity point can be shifted by as much as +51 V through simple thermal annealing of HSQ on top of EG. This shift corresponds to a change in the location of the Fermi level with respect to the Dirac point of $\sim$0.45 eV. The p-type doping is attributed to O provided by broken Si–O bonds in HSQ. This letter elucidates the detrimental effects to the p-type electrical transport properties, including a reduction in carrier mobility and a decrease in the $I_{\rm on}/I_{\rm off}$ ratio, a characterization lacking in previous spectroscopic studies of EG doping. Thermal annealing represents a blanket method of doping an entire sample, but local methods for individual devices can be envisioned by utilizing varying e-beam doses or current annealing, both of which would locally add energy to the HSQ thin film and result in similar p-type doping effects. The work presented here provides a technique for enabling p-n junction formation and CMOS functionality in EG.

References

[1] M. I. Katsnelson, K. S. Novoselov, and A. K. Geim, "Chiral tunneling and the Klein paradox in graphene," *Nat. Phys.*, vol. 2, no. 9, pp. 620–625, Sep. 2006.

[2] C. Berger, Z. M. Song, X. B. Li, X. S. Wu, N. Brown, C. Naud, D. Mayou, T. B. Li, J. Hass, A. N. Marchenkov, E. H. Conrad, P. N. First, and W. A. de Heer, "Electronic confinement and coherence in patterned epitaxial graphene," *Science*, vol. 312, no. 5777, pp. 1191–1196, May 2006.

[3] F. Varchon, R. Feng, J. Hass, X. Li, B. N. Nguyen, C. Naud, P. Mallet, J. Y. Veuillen, C. Berger, E. H. Conrad, and L. Magaud, "Electronic structure of epitaxial graphene layers on SiC: Effect of the substrate," *Phys. Rev. Lett.*, vol. 99, no. 12, p. 126 805, Sep. 2007.

[4] K. V. Emtsev, F. Speck, T. Seyller, L. Ley, and J. D. Riley, "Interaction, growth, and ordering of epitaxial graphene on SiC (0001) surfaces: A comparative photoelectron spectroscopy study," *Phys. Rev. B*, vol. 77, no. 15, p. 155 303, Apr. 2008.

[5] C. Riedl, C. Coletti, T. Iwasaki, A. A. Zakharov, and U. Starke, "Quasi-free-standing epitaxial graphene on SiC obtained by hydrogen intercalation," *Phys. Rev. Lett.*, vol. 103, no. 24, p. 246 804, Dec. 2009.

[6] B. Premlal, M. Cranney, F. Vonau, D. Aubel, D. Casterman, M. M. De Souza, and L. Simon, "Surface intercalation of gold underneath a graphene monolayer on SiC (0001) studied by scanning tunneling microscopy and spectroscopy," *Appl. Phys. Lett.*, vol. 94, no. 26, p. 263 115, Jun. 2009.

[7] S. Y. Zhou, D. A. Siegel, A. V. Fedorov, and A. Lanzara, "Metal to insulator transition in epitaxial graphene induced by molecular doping," *Phys. Rev. Lett.*, vol. 101, no. 8, p. 086 402, Aug. 2008.

[8] C. Coletti, C. Riedl, D. S. Lee, B. Krauss, L. Patthey, K. von Klitzing, J. H. Smet, and U. Starke, "Charge neutrality and band-gap tuning of epitaxial graphene on SiC by molecular doping," *Phys. Rev. B*, vol. 81, no. 23, p. 235 401, Jun. 2010.

[9] M. Y. Han, B. Ozyilmaz, Y. B. Zhang, and P. Kim, "Energy band-gap engineering of graphene nanoribbons," *Phys. Rev. Lett.*, vol. 98, no. 20, p. 206 805, May 2007.

[10] D. Estrada, S. Dutta, A. Liao, and E. Pop, "Reduction of hysteresis for carbon nanotube mobility measurements using pulsed characterization," *Nanotechnology*, vol. 21, no. 8, p. 085 702, Feb. 2010.

[11] H. Namatsu, T. Yamaguchi, M. Nagese, K. Yamazaki, and K. Kurihara, "Nano-patterning of HSQ resist with reduced linewidth fluctuations," *Micro. Eng.*, vol. 41/42, pp. 331–334, Mar. 1998.

[12] S. Ryu, M. Y. Han, J. Maultzsch, T. F. Heinz, P. Kim, M. L. Steigerwald, and L. E. Brus, "Reversible basal plane hydrogenation of graphene," *Nano Lett.*, vol. 8, no. 12, pp. 4597–4602, Dec. 2008.

[13] K. Brenner and R. Murali, "Single step, complementary doping of graphene," *Appl. Phys. Lett.*, vol. 96, no. 6, p. 063 104, Feb. 2010.

[14] C. C. Yang and W. C. Chen, "The structures and properties of hydrogen silsesquioxane (HSQ) films produced by thermal curing," *J. Mater. Chem.*, vol. 12, no. 4, pp. 1138–1141, Feb. 2002.

[15] M. P. Petkov, M. H. Weber, K. G. Lynn, K. P. Rodbell, and S. A. Cohen, "Open-volume defects in thin film hydrogen-silsesquioxane spin-on-glass; correlation with dielectric constant," *J. Appl. Phys.*, vol. 86, no. 6, pp. 3104–3109, Sep. 1999.

[16] S. E. Bryan, Y. Yang, and R. Murali, "Conductance of epitaxial graphene nanoribbons: Influence of size effects and substrate morphology," *J. Phys. Chem. C.*, vol. 115, no. 20, pp. 10 230–10 235, Apr. 2011.

[17] J. L. Tedesco, B. L. VanMil, R. L. Myers-Ward, J. M. McCrate, S. A. Kitt, P. M. Campbell, G. G. Jernigan, J. C. Culbertson, C. R. Eddy, and D. K. Gaskill, "Hall effect mobility of epitaxial graphene grown on silicon carbide," *Appl. Phys. Lett.*, vol. 95, no. 12, p. 122 102, Sep. 2009.

[18] J. H. Chen, C. Jang, S. Adam, M. S. Fuhrer, E. D. Williams, and M. Ishigami, "Charged-impurity scattering in graphene," *Nat. Phys.*, vol. 4, no. 5, pp. 377–381, May 2008.

[19] J. Yan, Y. B. Zhang, P. Kim, and A. Pinczuk, "Electric field effect tuning of electron–phonon coupling of graphene," *Phys. Rev. Lett.*, vol. 98, no. 16, p. 166 802, Apr. 2007.

[20] T. Fang, A. Konar, H. Xing, and D. Jena, "Carrier statistics and quantum capacitance of graphene sheets and ribbons," *Appl. Phys. Lett.*, vol. 91, no. 9, p. 092 109, Aug. 2007.